27th EPS Conference on Contr. Fusion and Plasma Phys. Budapest, 12-16 June 2000 ECA Vol. **24B** *(2000) 153 -156*

ExB flow shearing rate evaluation in JET ITB discharges

F. Crisanti, B. Esposito, L. Bertalot[1], C. Giroud[1], C. Gormezano[1], C. Gowers[1], R. Prentice[1], A. Tuccillo, K.-D. Zastrow[1], M. Zerbini[1]

Associazione Euratom-ENEA sulla Fusione, C.P 65, I-00044 Frascati (Roma), Italy
[1]JET Joint Undertaking, Abingdon, Oxfordshire OX14 3EA, UK

1. INTRODUCTION

The ExB flow shear [1] is thought to be responsible for the turbulence reduction linked with various improved transport regimes (H mod, VH mode, high l_i, Internal Transport Barrier (ITB)) observed in several tokamak experiments. In principle, the radial electric field E_r can be evaluated from the plasma radial force balance equation. In the framework of the neo-classical theory, this can be re-formulated by using the Ernst formula [2] as:

$$E_r = u_{\phi x} B_\theta + \frac{1-\alpha_1-\alpha_2/2}{1+\alpha_2}\frac{dT_i}{dr} + (1-\alpha_3)\frac{T_i}{n_i}\frac{dn_i}{dr} \qquad (1)$$

The electric field E_r can be evaluated from this equation even in experiments like JET where no direct measurements of the poloidal flow velocity are present; $u_{\phi x}$ and T_i are, respectively, the carbon impurity toroidal velocity and the plasma ion temperature; the poloidal magnetic field B_θ can be inferred from the EFIT equilibrium reconstruction code. For the ion density n_i no measurements are available, but an evaluation can be obtained if n_i is assumed to be proportional to some measured quantity, for instance the electron density, or the electron temperature. This approximation will be discussed in the following error analysis. The parameters α_i appearing in equation (1) are defined by linear combinations of the μ_i viscosity coefficients, which can be evaluated from the experimental data by using a rational approximation and their asymptotic values [3]. The ExB flow shearing rate ω_s is calculated according to the formula:

$$\omega_s = \left| \frac{RB_\theta}{B_\phi}\frac{\partial}{\partial r}\left(\frac{E_r}{RB_\theta}\right)\right| = \left| \frac{1}{B_\phi}\frac{\partial E_r}{\partial r} - \frac{E_r}{RB_\phi B_\theta}\left[\frac{\partial R}{\partial r}B_\theta + R\frac{\partial B_\theta}{\partial r}\right]\right| = \left| \frac{1}{B_\phi}\frac{\partial (u_{\varphi x}B_\theta)}{\partial r} + \left(\frac{1-\alpha_1-\alpha_2/2}{1+\alpha_2}\right)\frac{\partial^2 T_i}{\partial r^2}\right| +$$

$$+ \left| (1-\alpha_3)\frac{T_i}{n_i}\frac{\partial^2 n_i}{\partial r^2} - \frac{E_r}{RB_\phi B_\theta}\left[\frac{\partial R}{\partial r}B_\theta + R\frac{\partial B_\theta}{\partial r}\right]\right| = \left| \omega_s^{\nabla U} + \omega_s^{TEMP} + \omega_s^{DENS} + \omega_s^{ER}\right| \qquad (2)$$

which is valid in the plasma outer midplane [1]. So far, preliminary studies [4] have not shown that the ExB flow shearing plays a major role in JET ITB discharges. In this paper, we will present a detailed analysis of the uncertainties on both E_r and ω_s when these are calculated according to the formulae (1) and (2). It will be also shown that the ITB formation in JET is correlated with ω_s becoming higher than γ_{η_i}, a linear growth rate characterising the turbulence onset.

2. RADIAL ELECTRIC FIELD AND ExB FLOW SHEARING RATE

A database has been produced containing ITB discharges from the JET 1999 campaign. The neutron yield is found to increase linearly with the maximum of the ion temperature profile gradient (Fig.1a); moreover, this gradient scales almost linearly with the plasma toroidal rotation (Fig.1b). Such experimental evidence is an indication of the possible role played on the ITB by the radial electric field. Therefore, the Ernst formula has been used to determine the radial electric field in JET discharges. In the following, we present the results concerning the discharge 48994 (B_T = 2.5 T, I_p = 2.2 MA, NBI = 12 MW, ICRH = 5 MW). The calculated radial electric field E_r (solid line) is plotted in Fig. 2a at t = 45.6 s when the internal barrier

achieves its maximum. The figure also shows the various contributions to E_r: it can be noted that both the toroidal rotation and the ion temperature gradient terms contribute to the total E_r, while the effect of the ion density gradient term is almost negligible. Moreover, it is also evident that the largest contribution comes from the toroidal rotation, although the ion temperature gradient has an effect on the location of the maximum of E_r

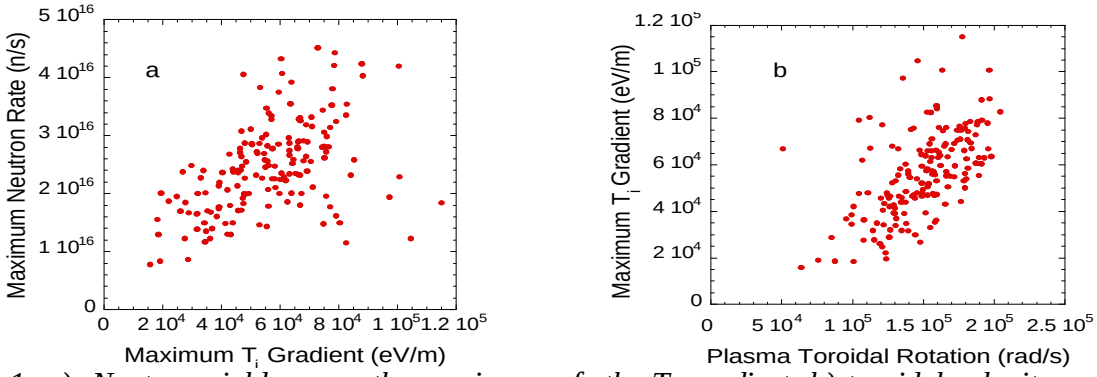

FIG. 1. a) Neutron yield versus the maximum of the T_i gradient; b) toroidal velocity versus the maximum of the T_i gradient

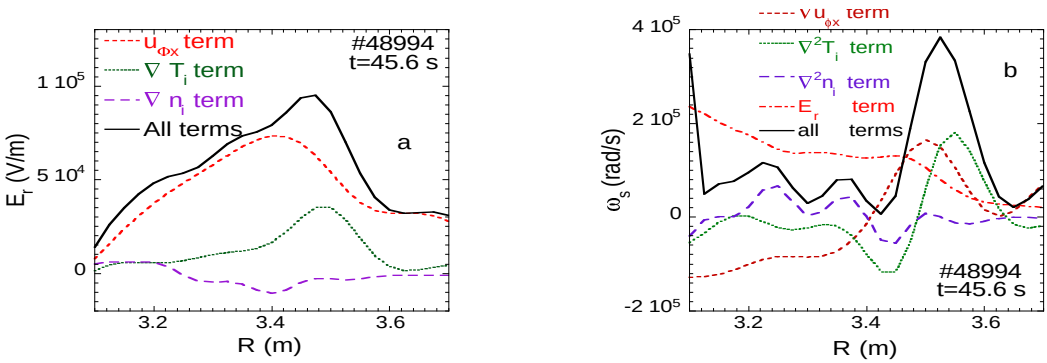

FIG. 2. a) E_r vs major radius R at fixed time: all terms defined in equation (1) are also shown.

b) ω_s versus major radius R at fixed time: all terms defined in equation (3) are also shown.

A similar analysis can be used in order to elucidate how the different physical quantities contribute to the E**x**B flow shearing rate ω_s.The four terms appearing in equation (2) are plotted vs major radius R in Fig.2b (again at t=45.6 s) together with the total E**x**B flow shearing rate ω_s (solid line). Several sources of errors must be taken into account when using the formulae (1) and (2) to evaluate E_r and ω_s. In the following, we will concentrate on the analysis of all experimental and computational errors, neglecting the errors due to the neoclassical theory approximation.

3. ERROR SENSITIVITY ANALYSIS

The main sources of errors on the determination of both E_r and ω_s can be summarised as follows: 1) assumptions in evaluating the ion density; 2) experimental errors on the measured profiles (T_i, n_e, B_{pol} and toroidal rotation); 3) limited radial resolution of the charge exchange spectroscopy diagnostic.

1) In all the calculations the ion density has been taken as a fraction of the electron density from LIDAR: $n_i(r)=n_e(r)/k_n$. An alternative estimate of $n_i(r)$ has also been obtained by normalising the electron temperature profile from reflectometry to the measured electron density, $n_i(r)=[T_e(r)/T_e(0)]n_e(0)/k_n$; in both cases k_n was chosen in the range 1÷3. In the case shown in

Fig.2a and Fig.2b $n_i(r)=n_e(r)/3$.The terms due to ion density are negligible and this is still true for all k_n values. The same result is obtained assuming $n_i(r)$ proportional to $T_e(r)$.

2) In order to take into account the experimental errors, both E_r and ω_s have been recalculated using the experimentally measured quantities perturbed by a random ±7.5% (which is larger than the experimental error on these quantities); this procedure has been carried out for each single variable and also for any combination of variables. Moreover, also different seeds for the random errors have been tried. For simplicity, only the worst case is reported here. In Fig. 3 a), b) are shown E_r and ω_s obtained by perturbing n_i and T_i: it turns out that the uncertainty on n_i and T_i mainly produces large errors on E_r and ω_s in the central plasma region, but only minor ones where the ITB is located. This is due to the fact that the experimental errors do not perturb too much the derivative terms of equations (1) and (2) in steep gradient regions.

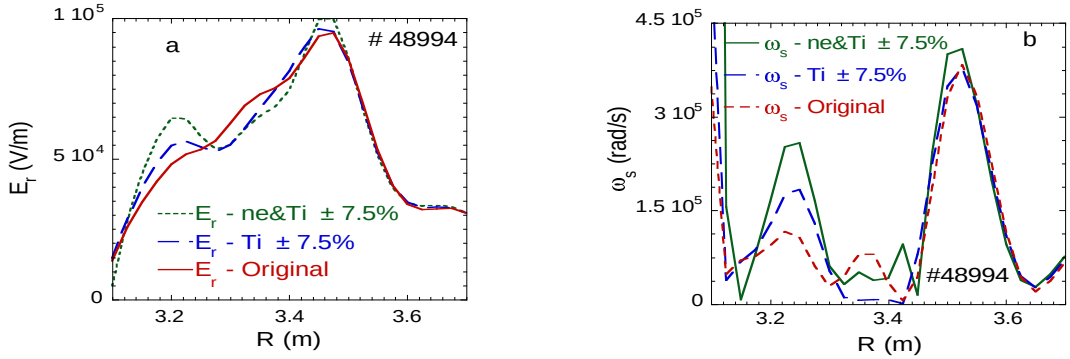

FIG. 3. Radial electric field (a) and shearing rate (b) calculated using the measured and the perturbed n_e and T_i profiles (t=45.6). All profiles are perturbed by random error of +/-7.5%.

3) As some interpolation of the experimental data is needed so that all the measured quantities are on the same spatial grid, artifacts can be introduced in the evaluated E_r and ω_s. The largest error is expected to arise from the ω_s^{TEMP} term, which contains the second derivative of the ion temperature; this term can produce a large contribution especially in the location of the ω_s maximum. The effects of using different spatial grids in the range R=3.0÷3.7 m has been studied by considering that the minimum number of radial points is given by the diagnostic with the minimum radial resolution (charge-exchange spectroscopy), while the maximum number of interpolating points can be fixed by assuming that the ion temperature cannot vary within an average ion Larmor radius. Again the experimental profiles can be still perturbed by random errors. In Fig. 4 we show ω_s obtained using a) the standard radial grid chosen for all the analysis presented in this paper (30 points similar to the EFIT one), b) the experimental charge-exchange radial grid (11 points) and c) a 120 points radial grid. For the case b) is plotted the minimum ω_s derived from the random error perturbed profiles. It can be noted that even in the most pessimistic case b), the qualitative features of the shearing rate in the ITB region do not change. In the central plasma region, where all the profiles are flat, the uncertainty in the ω_s evaluation becomes larger. To summarise: the general shearing rate behaviour can be determined in the ITB region independently on any strong pessimistic assumptions and experimental errors; however, the situation in the central plasma region is less clear and the errors can affect the final result. The central plasma is also the region where the magnetic shear may play an important role. To study this problem, the flat current density profile, as reconstructed by the EFIT equilibrium code for discharge #48994, has been modified into a very peaked or deeply hollow profile, all the other parameters being unchanged. In Fig.5 is shown the radial profiles of ω_s obtained using three different q profiles: a) the original EFIT profile; b) a modified q profile with the central $q \leq 1$; c) a hollow q profile with $q_{min}\approx 2$ and $q_o\approx 4$. These large variations in the q profiles do not affect the shearing rate behaviour; the conclusion is that, within the present experimental uncertainties, it is not possible to estimate the

effect of the magnetic shear in the shearing rate behaviour. The last point studied in the sensitivity analysis concerns the role played by the α_i coefficients used in the approximation of the poloidal velocity in the Ernst Formula. It can be noted in Fig.6, that by using α_3=0 (pure plasma approximation) the general trend of E_r does not change; on the contrary, if in equation (2) only the toroidal rotation and the ion density gradient terms are kept the main features in E_r are lost.

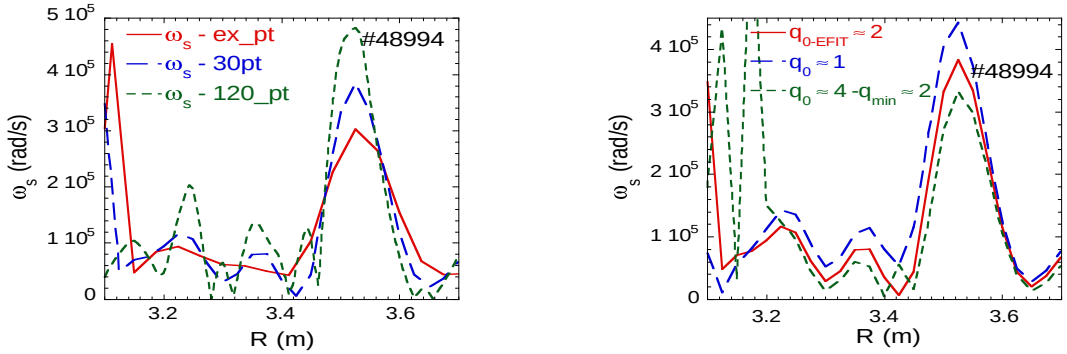

FIG. 4. ω_s obtained with three different grids of data interpolation. a) by using experimental charge-exchange points; b) the grid (35 points) used for the rest of this work; c) a grid(120 points) connected with the average ion Larmor radius.

FIG. 5. ω_s worked out by using three different q profiles. a) The standard one from EFIT; b) q profile with $q_{axis}\approx1$; q profile with $q_{axis}\approx4$ and $q_{min}\approx2$

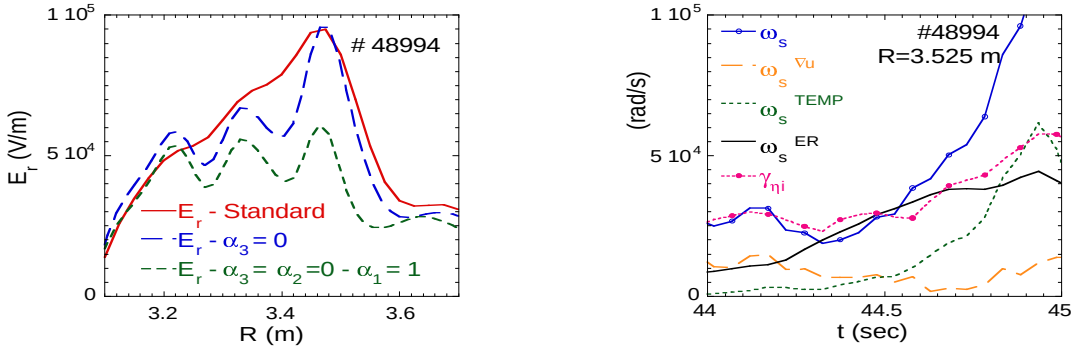

FIG. 6. E_r obtained by using different approximations for the poloidal velocity in Equation 2
FIG. 7. Shearing rate and linear growth rate plotted versus time at fixed plasma radius.

4. CONCLUSIONS

The onset of an ITB phase is found to be often correlated with the increase of the flow shearing rate ω_s over a linear growth rate characterising the ion temperature gradient (ITG) driven instability, γ_{η_i} [5]. In Fig. 7 γ_{η_i} is compared with the shearing rate ω_s (and its contributing terms as defined in equation (2)). It can be noted that the ω^{ER} term (the one dominated by the toroidal rotation) is increasing before of the ITB formation.As a main consequence it is possible that the toroidal velocity could be the trigger for the ITB formation in JET discharges [6].

REFERENCES

[1] BURREL, K. H., Phys. Plasmas **4**, 1499 (1997).
[2] ERNST, D. R., BELL, M. G., BELL, R.E., et al., Phys. Plasmas **5**, 665 (1998).
[3] KIM, Y.B., DIAMOND, P.H. and GROEBNER, R.J., Phys. Fluids B **3**, 2050 (1991).
[4] PARAIL, V.V., BALET, B., BARANOV, Y.F., et al., in Controlled Fusion and Plasma Physics (Proc. 26th Eur. Conf. Maastricht, 1999) P1.018, Vol.23J, p 181.
[5] NEWMAN, D.E., CARRERAS, B.A., LOPEZ-BRUNA, D., et al., Phys. Plasmas **5**, 938 (1998).
[6] CRISANTI, F., ESPOSITO, B., BERTALOT, L., et al., submitted to Nuclear Fusion.